Lab on a Chip

PAPER

View Article Online
View Journal | View Issue

Cite this: *Lab Chip*, 2021, **21**, 4652

High throughput production of microcapsules using microfluidics for self-healing of cementitious materials

Lívia Ribeiro de Souza * and Abir Al-Tabbaa

Capsule-based self-healing of cementitious materials is an effective way of healing cracks, significantly extending the life of structures, without imposing changes due to the incorporation of capsules into products during mixing. The methodologies currently being used for the development of capsules with a liquid core as a healing agent yield a wide range of sizes and shell thicknesses for the microcapsules, preventing a detailed assessment and optimisation of the microcapsule size and its effects. Uniquely, microfluidic technology offers precise control over the size and shell thickness through the formation of double emulsions. The drawback is that only small quantities of material can be typically produced. Here, by using paralleled junctions in a microfluidic device, high throughput production of materials was achieved, focusing for the first time on self-healing of cementitious materials. A microfluidic chip was assembled with 4 channels in parallel and selected hydrophobicity for the formation of the double emulsions. A coefficient of variation below 2.5% was observed for the 4 junctions, demonstrating the formation of monodisperse capsules. The control over the size and shell thickness by adjusting the flow rates was demonstrated, yielding capsules with an outer diameter of 615–630 μm and a shell thickness varying between 50 and 127 μm. By using triethanolamine as a surfactant, capsules with an aqueous core were produced. Furthermore, by selecting PEA, an acrylate with low tensile strength, the capsules embedded in the cement paste were successfully triggered to release the healing agent by crack formation. Capsules were successfully produced continuously for 7 h, with inner and outer diameters of 500 ± 31 μm and 656 ± 9 μm at a production rate of ~13 g h^{-1} and a yield of around 80%. With these results and considering up to 6 chips in parallel, the production rate could be up to 1.5 kg per day. This demonstrates the huge potential of the microfluidic device with unique features to produce sufficiently large quantities of microcapsules for laboratory-scale assessment of self-healing performance.

Received 26th June 2021,
Accepted 17th October 2021

DOI: 10.1039/d1lc00569c

rsc.li/loc

Introduction

Inspired by the healing processes that occur in nature, the concept of self-healing of cementitious materials aims at decreasing repetitive and extensive maintenance cycles needed in infrastructures as well as extending their service life significantly contributing to the delivery of net zero by 2050.[1] The occurrence of cracks in a cementitious infrastructure facilitates the ingress of water and chlorides which results in corrosion of the reinforcing steel, causing deterioration in concrete.[2] With the use of self-healing in concrete, when cracks are formed in the matrix, the healing takes place without the need for any external intervention.[3] This leads to the recovery in the transport properties and hence the durability performance and, to some extent, the recovery in the mechanical properties. Several methodologies have been applied to achieve such self-healing, including the enhancement in the autogenous capacity of cementitious materials to heal their own cracks through the addition of minerals,[4,5] fibres,[6] and superabsorbent polymers (SAPs),[7] and autonomic healing through vascular systems,[8,9] bacteria[10–12] and shape memory polymers.[13] However, the addition of these materials may lead to unwanted variations in the rheology during mixing and/or burdensome changes during casting.[14] Capsules for self-healing of cementitious materials, on the other hand, can easily be added during the mixing of cement and, at lower concentrations, have minimum effects on the mixture.[15,16] Once a crack is formed, the damage act as a trigger for releasing the encapsulated material. When the healing agent is released, it reacts and fills the crack, minimising the damage.[17] Examples of encapsulated healing agents for cementitious materials include liquids such as epoxy[18] and dissolved or emulsified minerals[19–21] and bacterial spores.[12] These materials have successfully been used to heal cracks up to 1 mm.[12]

Department of Engineering, University of Cambridge, Cambridge CB2 1PZ, UK.
E-mail: lrds2@cam.ac.uk

A widely used strategy to produce capsules with liquid cores in large quantities is bulk emulsification followed by polymerisation of the shell. This methodology has been successfully used to encapsulate healing agents with a wide range of shells, such as poly(urea-formaldehyde),[22] polyurea,[16,23] gelatine-gum arabic,[21] melamine formaldehyde,[12] and others. However, the inherent limitation of such a bulk method is the production of capsules with a range of sizes,[24–26] shell thicknesses and structures, thus offering poor control of their release properties. Overall, ideal capsules should present suitable tensile strength and a good interfacial bond with the cementitious materials, as they would be easily triggered by cracks.[27] Other functionalities can also be programmed within the shell composition to create delivery systems whose release is controlled by variations in the pH and chloride concentration and ultrasonic triggering.[28–30]

In the past few years, microfluidic production of double emulsions has gained attention due to their precise control over the size and shell thickness of the capsules, as well as a wide variety of shell properties.[31] However, the small scale of the chips and the low flow rates limit their large-scale production. For one single chip, the flow rates are typically around 0.5–1 g h^{-1} for the production of microcapsules.[31,32] These throughput values limit the number of tests performed with the microcapsules. Particularly for self-healing of cementitious materials, a full spectrum of tests to evaluate the performance of capsules for the self-healing of cementitious materials, including the capsule concentration, compressive strength, rheology, permeability and crack healing at different contents of microcapsules, would need approximately 300 g of material.[15,16] To scale up the production, paralleled junctions in a microfluidic device have been explored, with early results placing 15–40 drop-makers consecutively to produce double emulsions.[33,34] However, for the reliable formation of water-in-oil-in-water double emulsions, a special pattern of wettability is necessary; in this case, a hydrophobic channel is used to form the water-in-oil emulsions, followed by the use of a hydrophilic channel for the double emulsion. Early studies circumvented the wettability issue by a selected change of geometry which allowed the hydrodynamic focusing of the middle phase.[33] In this case, the flow rates of middle and continuous phases are limited. Alternatively, emulsions with a core comprised of gas or with a core similar to the shell have also been investigated, as their production does not depend on the selected surface wettability.[34,35] Recent advances on microfluidic systems have been used for larger-scale production of water-in-oil-in-water emulsions, producing up to ~50 g h^{-1}.[36,37] Furthermore, a combination of large-scale production and machine learning can be used to minimise the need for a human operator checking the continuous production.[38,39]

Here, the high throughput production of microcapsules using microfluidics for mechanically triggered self-healing in the cementitious matrix was investigated. A microfluidic chip was developed with four junctions in parallel and suitable wettability for the formation of double emulsions. To demonstrate the monodisperse formation of double emulsions, the coefficient of variation between the double emulsions formed at the four junctions was investigated. Furthermore, the control over the size and shell thickness of the double emulsions was demonstrated. The double emulsion template was then used to produce capsules containing aqueous and organic cores. In addition, capsules comprised of a shell with a low tensile strength and good interfacial bond with the cementitious matrix were produced. In addition, capsules were produced continuously for 7 h, demonstrating the fabrication of sufficient materials for laboratory-scale testing of self-healing performance. The size, shell thickness, core retention and yield of the continuous production were characterised. This study demonstrates the possibility of high throughput generation of microcapsules with a controlled size and shell thickness for lab-scale assessment of self-healing performance in cementitious matrixes.

Results and discussion

Design of the chip

The double emulsion template used for the formation of microcapsules was produced using a microfluidic chip, as illustrated in Fig. 1. During the design of the chip, four main factors were considered: (i) the selected pattern of wettability, allowing the production of water-in-oil-in-water double emulsions; (ii) the uniform distribution of flow across each microfluidic junction; (iii) the size of the double emulsions which is ~500–600 μm, as this size is suitable for self-healing of cementitious materials; and (iv) the largest number of junctions possible in a single chip for maximised production. For the production of double emulsions with an aqueous (or organic) core and an organic middle layer, the chip is composed of two parts connected together by a gasket: the first half has hydrophobic coating; after the gasket, the second part is glass, *i.e.*, a hydrophilic material. In this way, the wettability of the chip was adapted to the production of water-in-oil-in-water double emulsions. The uniform distribution of liquids over the droplet generators connected to a single distribution channel is achieved when the distribution channel is large enough so that the flow resistance R_D along the channel must be negligible compared to the flow resistance R_J through the microfluidic junction.[33] The resistance of a rectangular channel can be calculated using $R = 12\ \mu L/wh^3$ and the resistance of a circular channel can be calculated using $R = 8\ \mu L/\pi a^4$, where μ is the dynamic viscosity of the fluid, and l, w, h and d are the length, width, height and diameter of the channel, respectively. Resistors were added to the inner, middle and outer channels, as described in the Experimental section; thus the presence of four junctions in the chip allows a uniform distribution of liquid over the chip. For the size of the double emulsions, it has been shown that the size of the droplets produced by flow focusing is comparable with the dimensions of the

opening.[40] Thus, the second junction was etched with a 500 μm height and a 510 μm width. Finally, considering the presence of the resistors, the width of the channels and the size of the clamps used in the commercially available Telos platform, the maximum number of junctions per chip was four. An advantage of this modular approach is the investigation of double emulsion production on a smaller scale (*i.e.*, one single chip with four junctions), as well as the easy scale-up of the production. In this case, the channel dimensions play an important role in the uniform distribution of liquids throughout the different channels. Considering the dimensions of the channel on the commercially available Telos platform and the resistors present in the chip, a system of linear equations can be used to describe the flow rates in this ladder geometry, with 4 junctions branching out from each channel. In this case, for a system with N chips, the ratio of flow rates between Q_N and Q_0 is described in eqn (1):

$$\frac{Q_N}{Q_0} = 1 - \frac{4R_D}{R_f}\frac{(N-1)N}{2} \quad (1)$$

Considering the design criteria that $Q_N/Q_0 \approx 0.99$, a maximum of 6 chips in parallel could be used with the chip presented in this work. To increase the value for N, the dimensions of the flow resistors and distribution channels may be tailored accordingly.

Double emulsion formation

The size and shell thickness of the monodisperse double emulsion is easily fine-tuned according to the flow rates used for the inner, middle, and outer phases. Considering the mechanism of formation of double emulsions in the dripping regime, the capillary number describes the main forces involved,[41] and the flow rates are the principal variables. Mineral oil was used as the inner fluid, ethylene glycol phenyl ether acrylate (PEA) was used as the middle fluid, and PVA 5 wt% was used as the outer fluid, using flow rates of 130, 32 and 430 μL min^{-1}, respectively, as shown in Fig. 2A. Highly monodispersed oil-in-oil-in-water double emulsions were formed in all four junctions with an outer diameter of 582 ± 4 μm for junction 1, 604 ± 6 μm for junction 2, 581 ± 5 μm for junction 3 and 602 ± 6 μm for junction 4. For each junction, the coefficient of variance (CV) was below 1%. The outer diameter for the 4 junctions combined was 590 ± 12

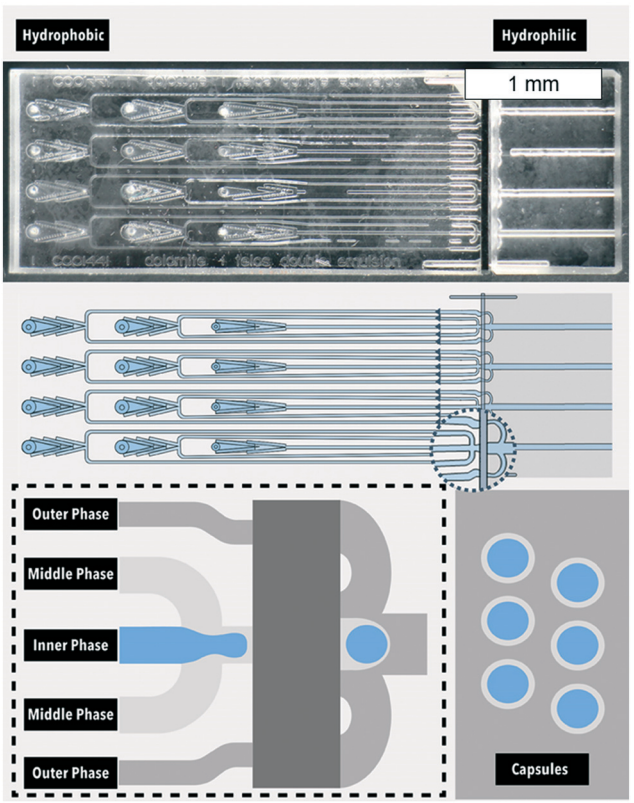

Fig. 1 A single microfluidic device for the generation of monodisperse double emulsion. (Top) Photograph of the microfluidic device with a gasket separating the hydrophobic channels in the first half and hydrophilic channels in the second half. (Middle) Schematic representation of a single microfluidic chip with four channels in parallel. (Bottom left) Flow focusing junction where the inner, middle and outer phases form double emulsions. (Bottom right) Microcapsules created by polymerising the double emulsion template.

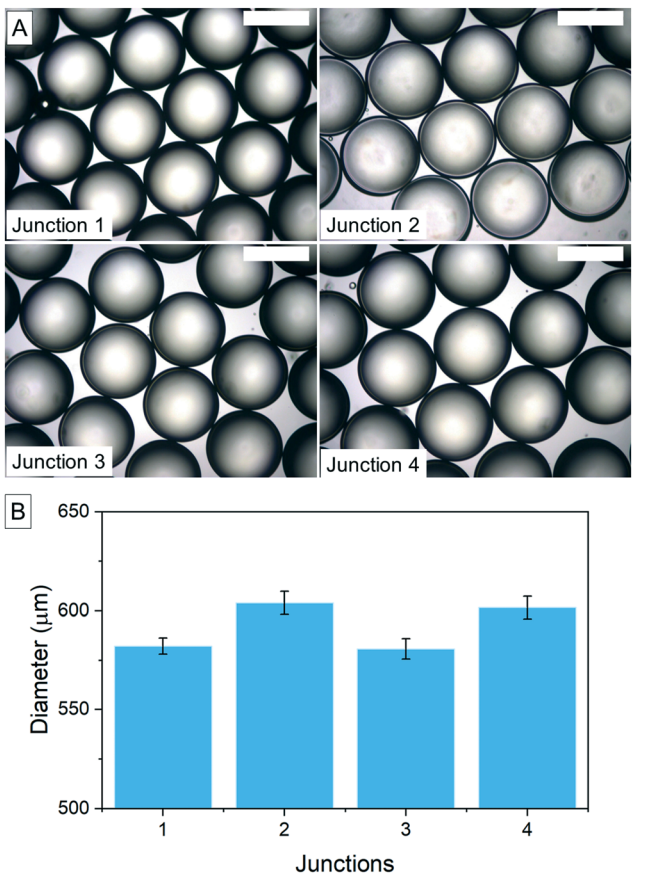

Fig. 2 (A) Optical microscopy image of double emulsion template for capsules with an organic core produced in the four paralleled junctions of the microfluidic device at a flow rate of 130, 32 and 430 μL min^{-1} for the inner, middle and outer fluids. Scale bar indicates 500 μm. (b) Outer diameter of the capsules produced at different junctions.

μm, with a CV below 2%, indicating the successful production of monodisperse double emulsions across the four junctions. The increase in CV for the combined junctions compared with the individual ones indicates small fluctuations in the flow rate distribution between the junctions. The shell thickness of 24 ± 2 μm was obtained by measuring the difference between the inner and outer diameters.

The relative shell thickness (h) is defined as a function of the flow rate of the inner (q_{inner}) and middle (q_{middle}) phases. By varying the flow rate of the inner phase, the shell thickness of the double emulsion can be defined as eqn (2):

$$h = \frac{D_{outer} - D_{inner}}{D_{outer}} = 1 - \left(1 + \frac{q_{middle}}{q_{inner}}\right)^{-1/3} \quad (2)$$

where D_{outer} is the outer diameter of the double emulsion and D_{inner} is the inner diameter.[41,42] The flow rate of mineral oil varied between 30 and 180 μL min^{-1} whilst the flow rate of PEA was kept constant at 123 μL min^{-1}. The optical microscopy images of the double emulsions produced in all four channels were measured, and the outer diameter and inner diameter are shown Fig. 3. The outer diameter for all the double emulsions varied between 615 to 630 μm with a coefficient of variation of ~5% for all samples. The outer diameter is mainly determined by the outer flow rate, which was kept constant at 400 μL min^{-1}. The inner diameter varied between 360 and 530 μm, with a shell thickness varying between 50 and 127 μm. A mean microcapsule diameter of around ~500–600 μm has been successfully demonstrated to be effective for self-healing of cementitious materials.[15,16] Thus, producing double emulsion templates in this range of size is suitable for self-healing. Furthermore, the fine-tuning of the shell thickness can be used to increase the probability of physical triggering.

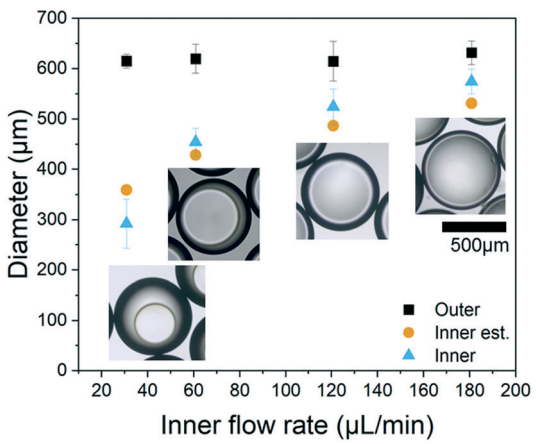

Fig. 3 Inner and outer diameters of the double emulsions at a constant middle flow rate of 123 μL min^{-1}, an inner flow rate varying between 30 and 180 μL min^{-1}, and a constant outer flow rate of 400 μL min^{-1}.

Production of microcapsules with an aqueous core

Capsules with an aqueous core were produced using the microfluidic set-up, as aqueous cores are fundamental for several mechanisms of self-healing in cementitious matrices.[17,43] Water-in-oil-in-water (w/o/w) double emulsions were produced using a mixture of triethanolamine in water as the core, trimethylolpropane ethoxylate triacrylate as the middle phase and PVA 5 wt% as the outer phase. Fig. 4A presents a typical optical microscopy image of the monodisperse double emulsions with an outer diameter of 597 ± 3 μm and an inner diameter of 522 ± 2 μm. The flow rates were 60, 30 and 300 μL min^{-1} for inner, middle and outer fluids, respectively. Triethanolamine contributed to an increase in the viscosity of the inner fluid, thus increasing the drag of the inner phase and facilitating the formation of double emulsions. In addition, it also acted as a nonionic surfactant, reducing the interfacial tension between the core and the acrylate phase and stabilising the double emulsions. The double emulsions were polymerised and collected in a flask containing PVA 5 wt%, immediately after the production. This is relevant to prevent the escape of the core during polymerisation. Fig. 4B shows the formed microcapsules with a clear core–shell structure. Furthermore, the density of triethanolamine increased the density of the core, minimising the effects of mismatched density that may lead to off-centred cores using microfluidics.[44]

The maximum throughput for the production of the double emulsions is dictated by the flow rates of the inner and middle fluids; however, it is also limited by the stability of the fluids. This is demonstrated with the water-in-oil-in-water double emulsion with PEA as the middle layer and PVA 5 wt% as the outer liquid. To form the double emulsions, the inner and middle fluid flow rates were varied between 55–210 μL min^{-1} and 30–150 μL min^{-1}, respectively. The thickness of the middle layer increased with the increase of the middle fluid flow rate, as shown in the optical microscopy images in Fig. 5. In contrast, the thickness of the middle layer decreased with the increase of the inner fluid flow rate. The double emulsion throughput varied according to the used flow rates, ranging between 6 to 20 g h^{-1} for a single chip. This value is comparable with recent reports in the literature, in which double emulsions were produced at a rate of 20 mL h^{-1}.[37] However, using a modular platform, more chips may be placed in parallel, and this system allows a 6-fold increase

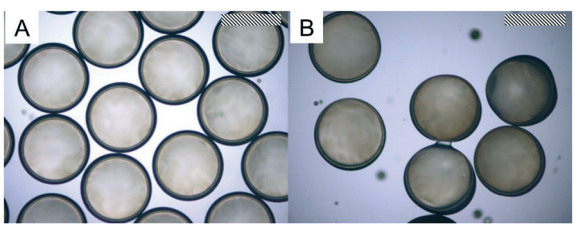

Fig. 4 Double emulsions (A) and capsules (B) produced with the water-in-oil-in-water double emulsion. Scale bar represents 500 μm.

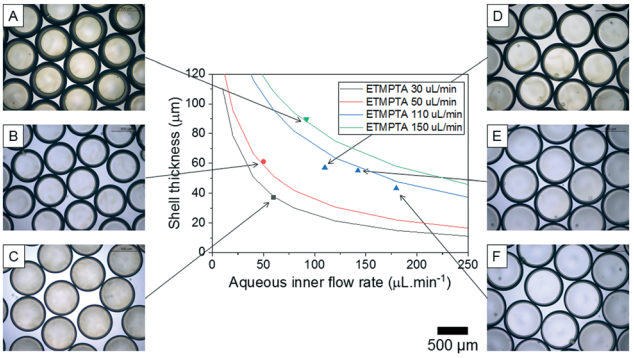

Fig. 5 Shell thickness of the water-in-oil-in-water (w/o/w) double emulsions tuned by controlling the inner and middle flow rates. The continuous black line indicates the estimated thickness of the middle layer for middle flow rates of 30 μL min^{-1} and outer diameter (OD) of 597 μm (Fig. 5C); the continuous red line represents the middle flow rates of 50 μL min^{-1} and OD of 560 μm (Fig. 5B); the continuous blue line represents the middle flow rate of 110 μL min^{-1} and OD of 662 μm (Fig. 5D–F); and the continuous green line represents the middle flow rate of 150 μL min^{-1} and OD of 633 μm (Fig. 5A). Symbols represent the measured middle layer thickness for double emulsions produced at a constant outer flow rate of 300 μL min^{-1}. Scale bar represents 500 μm.

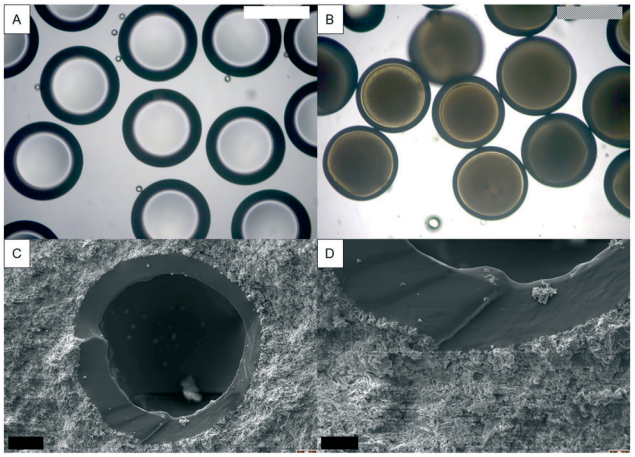

Fig. 6 Microcapsules produced for the physical triggering of self-healing in the cementitious matrix. A) Optical image of the double emulsions with mineral oil as the core and PEA as the shell. Scale bars: 500 μm. B) Optical image of the microcapsules after the photopolymerisation of PEA. Scale bars: 500 μm. C and D) SEM images of the microcapsules embedded in the cement paste. Scale bars: 100 μm and 50 μm for C and D, respectively.

in the production. At flow rates of 60 and 30 μL min^{-1} for inner and middle fluids, double emulsions were formed at the cross junction of the microfluidic channel in the dripping regime. With the increase of the inner and middle fluid flow rates, the throughput increases, and the droplet formation changes to the jetting and threading regimes,[45,46] still robustly forming double emulsions. At inner flow rates above 150 μL min^{-1} (for a middle flow rate of 110 μL min^{-1}), the stability of the system was significantly reduced and the double emulsions are unlikely to be formed. Thus, aiming at a high throughput, thinner shells, and stable formation of double emulsions, inner and middle fluid flow rates ranging from 60–120 μL min^{-1} and 30–110 μL min^{-1}, respectively, were preferred.

Production of microcapsules with the shell for physical triggering

For physical triggering when a crack is formed, the microcapsules need to exhibit a good interfacial bond with the cement paste and a low tensile strength to allow the rupture of the shell. Ethylene glycol phenyl ether acrylate (PEA) was selected as the acrylate for photopolymerisation into the shell due to its good interfacial bonding with cementitious materials and low tensile strength (~0.4 MPa).[47] The PEA shelled microcapsules were produced using mineral oil as the core, PEA as the shell and PVA 5 wt% as the outer material. Whilst the outer flow rate was kept constant at 400 μL min^{-1}, the inner and middle flow rates were 90 and 150 μL min^{-1}, respectively. The resulting double emulsion was produced with an outer diameter of 600 μm and a shell thickness of 90 μm (Fig. 6A). Fig. 6B shows the capsules collected in a solution of PVA 5 wt% whilst being polymerised on the fly, at a production rate of ~14 g h^{-1}. As the capsules are mostly comprised of PEA, an acrylate with a density of 1.1 g L^{-1}, the material drops instead of floating. This means that the material does not agglomerate. Then the material was cast in the cement paste – w/c at 0.45. After cracking, the capsules ruptured and released the mineral oil core, as observed with a stereoscope. In addition, the scanning electron microscopy images show a very good bond between the capsule and the cement matrix, as shown in Fig. 6C and D. And all capsules embedded in the cement ruptured upon crack formation. A previous investigation on the encapsulation and behaviour in cement of capsules with ethylene glycol phenyl ether methacrylate and ethylene glycol phenyl ether acrylate revealed that acrylates present a good interfacial bond with a cement paste once compared with the methacrylates with the same moieties. This hints at the importance of the structure of PEA that allows a good interfacial bond with a cement paste.

High throughput production of microcapsules

The production of large quantities of microcapsules is essential for lab assessment of the capsule-based self-healing performance of materials. To demonstrate the use of paralleled junctions for the continuous production of double emulsions, microcapsules with PEA as the shell and mineral oil as the core were produced for 7 hours. Mineral oil, PEA and PVA 5 wt% were pumped at constant flow rates of 82, 130 and 400 μL min^{-1}, respectively. Double emulsions were successfully formed in the dripping regime at the cross junction, as shown in Fig. 7A. The formed double emulsions are shown in the optical microscopy image in Fig. 7B, and the histograms indicating the size distributions are shown in Fig. 7E. For these flow rates, the typical inner and outer diameters were 500 ± 31 μm and 656 ± 9 μm, with a

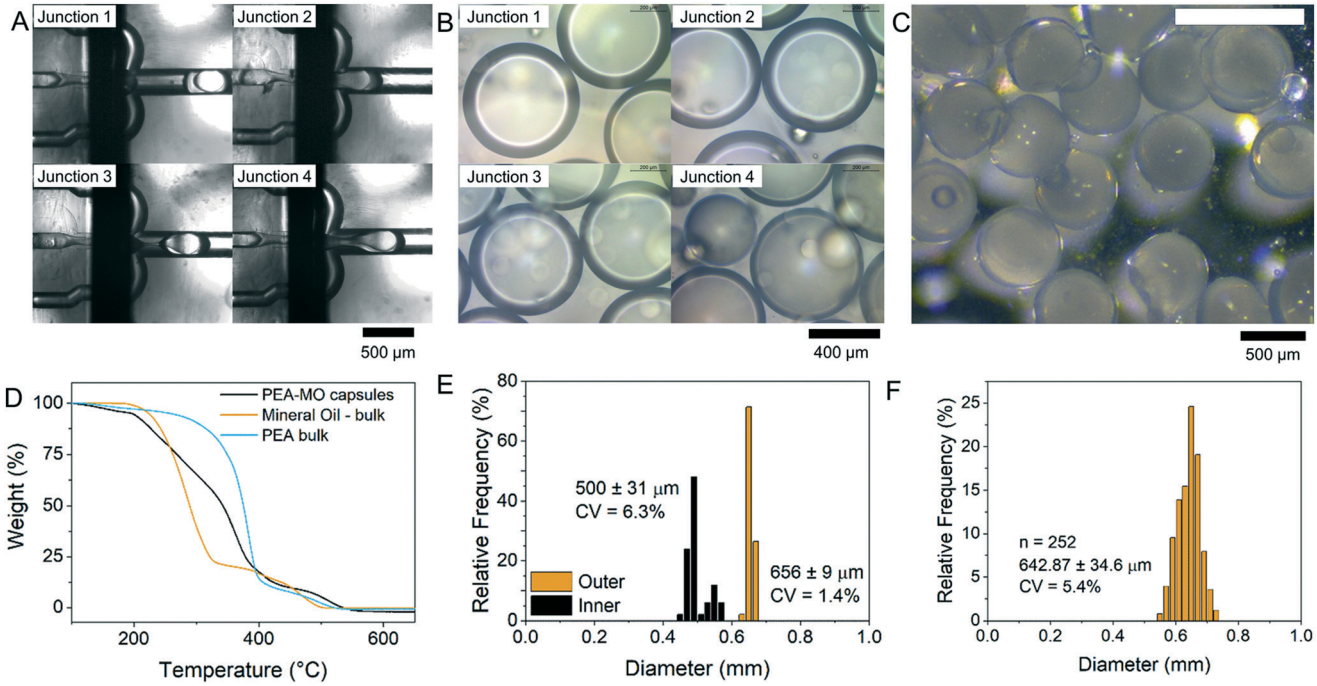

Fig. 7 Double emulsion templates continuously formed for the production of microcapsules. (A) Optical microscopy image of the four microfluidic junctions in parallel producing double emulsions at flow rates for the inner, middle and outer phases of 82 µL min^{-1}, 130 µL min^{-1} and 400 µL min^{-1}, respectively. Scale bar represents 500 µm. B) Optical microscopy image of the oil-in-oil-in-water double emulsion produced using junctions in parallel. Scale bar represents 400 µm. (C) Stereoscopy image of the microcapsules formed after photopolymerisation. Scale bar represents 1000 µm. D) TGA indicating the core retention. E) Size distribution of the outer diameter of the microcapsules, collected over 7 h of reaction. F) Size distribution of the inner and outer diameters of the double emulsions.

coefficient of variation of 6.3 and 1.4%, respectively. The increase in the CV for the inner flow rate was attributed to inhomogeneous distribution of the inner phase across the parallel junctions. The presence of inbuilt filters, whilst successfully hindering the occlusion of the junctions with debris, can also cause preferential flow rates in certain junctions over others. Fig. 7C shows a stereoscopy image of the microcapsules formed after the polymerisation. The double emulsions and the microcapsules are denser than the solution of PVA 5 wt% used to collect the material, and therefore, it sinks during the polymerisation. Furthermore, no agglomeration of the capsules was observed. The size distribution of the capsules obtained for 7 h is slightly broader than those obtained for shorter periods of time. This increase in the size distribution is attributed to small variations in the flow rate over time and the inhomogeneous distribution of the fluid phases across the parallel junctions. Nevertheless, we find parallel operations to yield good uniformity, with a CV for the outer diameter of ~5.4% (Fig. 7F). For these flow rates, the total throughput defined as the sum of the inner and middle phases is 12.72 mL h^{-1} or 13.04 g h^{-1}. By filtering the collected capsules after the production, the production yield was estimated to be 81 ± 1%. The main reason behind a yield lower than 100% is the mismatched density between the inner and middle fluids, leading to a displacement of the core before the polymerisation. As a result, some of the capsules have a bowl-like shape, where the core escapes during polymerisation. This was also confirmed by thermogravimetric analysis (Fig. 7D), in which the amount of mineral oil retained inside the capsules was estimated to be 44 ± 21%. This equates to a production rate of 84.5 g in 8 h, *i.e.*, working hours, and ~0.25 kg per day. By paralleling more microfluidic chips in the same platform, a further increase in the production rate is possible. We estimate that a device containing 6 microfluidic chips in parallel, each one containing 4 junctions, could generate double emulsions at a rate of 1.5 kg per day.

Conclusions

High throughput production of microcapsules using microfluidics was successfully carried out for self-healing of cementitious materials. A microfluidic chip was designed in glass, with 4 channels in parallel. The modular approach enables the change in wettability for the production of double emulsions. Highly monodisperse double emulsions are formed using the channels in parallel, with a coefficient of variance below 2.5%. By varying the inner and middle fluid flow rates, the shell thickness was successfully tailored to produce capsules with an outer diameter of ~600 µm and a shell thickness between 50 and 127 µm. Furthermore, the flow rates were in the range of 30–180 µL min^{-1} for the inner fluid and 32–120 µL min^{-1} for the middle fluid, resulting in a production rate of 6–20 g h^{-1}. Capsules with an aqueous core were produced using triethanolamine as the surfactant.

Aiming at physically triggered self-healing, capsules with ethylene glycol phenyl ether acrylate (PEA) as the shell material were produced, given its low tensile strength. The capsules also showed very good interfacial bonding with the cement, and capsule-based self-healing was triggered by the crack formation. For the production of capsules for lab scale tests for self-healing, capsules were produced continuously for 7 h. The inner and outer diameters of the double emulsions were 500 ± 31 μm and 656 ± 9 μm, respectively. The coefficient of variation for the outer diameter of the capsules produced over 7 h was 5.4%, and the encapsulation yield was 81%.

The paralleled channels markedly amplify the production rate of double emulsions, without compromising the uniformity. By the addition of more microfluidic chips in parallel, we can further increase the throughput. This platform enables the production of emulsions for lab scale tests for self-healing.

Experimental

To produce the double emulsion, a microfluidic device with four flow-focusing channels in parallel was placed in a Telos device (Dolomite Microfluidics, UK), as shown in Fig. 1. To obtain the suitable wettability for the production of double emulsions, the first part of the chip is hydrophobic while the second part is hydrophilic with a gasket connecting the two parts. At the first junction, where the inner flow is in contact with the middle flow, the junction is 300 μm deep and 310 μm wide. At the second junction, where the outer flow engulfs the previous two, the junction is 500 μm deep and 510 μm wide. The channel for the inner flow rate was 11.5 mm long, 240 μm wide and 80 μm deep; each of the 2 channels for the inlet of the middle flow was 20 mm long, 170 μm wide and 80 μm deep; and each of the 2 channels for the inlet of the outer flow was 27.5 mm long, 170 μm wide and 80 μm deep. In addition, the design also includes two sets of filters as a trapping point for debris, the first one with a depth of pores of 80 × 170 μm and the second set with a depth of pores of 47 × 130 μm. The Telos platform is modular and composed of different modules being clamped together. The main inflow pathway presents a diameter of 1.5 mm and a length of 27 mm (for each module) and branches out for individual modules through channels with a length of 23.5 mm and a diameter of 1.0 mm. The inner fluid was injected using a syringe pump (Aladdin AL-1000) at the range of flow rates of 30–210 μL min^{-1}; the middle and outer fluids were injected using pressure pumps (Dolomite Microfluidics, UK) at typical flow rates of 30–150 μL min^{-1} and 300–430 μL min^{-1}, respectively. Double emulsions with an organic core were formed using mineral oil (light, Sigma Aldrich, density of 0.838 g mL^{-1}, viscosity 29.3 mPa s). For the aqueous core, a solution of triethanolamine (Sigma Aldrich) in water (1 : 1) was used as the inner phase. The monomers used as the precursor of the shell in the middle phase were trimethylolpropane ethoxylate triacrylate (ETMPTA, Sigma Aldrich, density 1.11 g mL^{-1}, viscosity 73.3 mPa s) and ethylene glycol phenyl ether acrylate (PEA, Sigma Aldrich) both containing 1 wt% of the photoinitiator hydroxy-2-methylpropiophenone. For the outer/continuous phase, an aqueous solution with 5 wt% poly(vinyl alcohol) (PVA, MW 13 000–23 000, 87–89% hydrolysed, viscosity 4.99 mPa s) was used. The polymerisation of the shell took place *via* UV-light (Omnicure, 50% opening) exposure over the collection tube shortly after the formation of the double emulsion droplets to minimise the effect of the density mismatch between the core and shell.[44] The resultant microcapsules were collected in an aqueous solution of 5 wt% PVA solution to prevent the agglomeration of the microcapsules during the polymerisation. To calculate the yield during the 7 h producing capsules, after every 1 h, the container with capsules under UV light was removed and replaced by a new container with PVA 5 wt%. The capsules were filtered (filter paper no. 1, pore size 2.5 μm, diameter 42.5 mm, Whatman) and washed with water to remove any excess PVA. The filtered material was then dried at room temperature for 24 h, and the weight of the dried material was measured. To investigate the yield, the weight of the dry capsules was divided by the sum of the weight of the inner and middle phases pumped for 1 h (calculated from the flow rates and density of the solutions). As this step was repeated every hour, an average yield was calculated for the 7 h of production. The outer and inner diameters of the produced double emulsions and microcapsules were measured with an optical microscope (OM) (DM 2700 M, Leica, Germany) and a stereoscope (Leica, Germany). To assess the thermal stability and oil content, the microcapsules, mineral oil and polymerised ethylene glycol phenyl ether acrylate beads were analysed using thermogravimetric analysis (TGA, PerkinElmer STA6000) between 50 and 700 °C at a rate of 5 °C min^{-1}, in an air atmosphere. For the investigation of the behaviour of the microcapsules in the cement paste, the microcapsules produced with mineral oil as the core and polymerised PEA as the shell were mixed with ordinary Portland cement (CEM I 42.5, provided by Heidelberg-UK) and water (w/c = 0.45). The mixture was then cast in oiled silicone moulds (10 × 10 × 50 mm^3). After 28 days of curing, the samples were broken, where it was possible to see the oil coming out of the microcapsules leaking to the sample. To investigate the interfacial bonding between the capsule and cement paste, a scanning electron microscope (SEM, Evo LS15, Zeiss) was used.

Author contributions

AA, LS – conceptualisation; LS – data curation, formal analysis, methodology, visualisation, and writing; AA – resources and supervision.

Conflicts of interest

There are no conflicts to declare.

Acknowledgements

Financial support from the EPSCR-funded project Resilient Materials for Life (RM4L – EP/P02081X/1) is gratefully acknowledged. The discussions with Phil Homewood (Dolomite, UK) and Paulo Strobel (Cranfield University) are also kindly acknowledged. The authors would like to thank Hiske Overweg (Microsoft) and her team for producing a platform to measure the double emulsions dimensions.

References

1 N. De Belie, E. Gruyaert, A. Al-Tabbaa, P. Antonaci, C. Baera, D. Bajare, A. Darquennes, R. Davies, L. Ferrara, T. Jefferson, C. Litina, B. Miljevic, A. Otlewska, J. Ranogajec, M. Roig-Flores, K. Paine, P. Lukowski, P. Serna, J.-M. Tulliani, S. Vucetic, J. Wang and H. M. Jonkers, *Adv. Mater. Interfaces*, 2018, 1800074.
2 P. K. Mehta and P. J. M. Monteiro, *Concrete: Microstructure, Properties, and Materials*, McGraw-Hill Education, 4th edn, 2014.
3 S. van der Zwaag, in *Self-Healing Materials*, ed. S. van der Zwaag, Springer Series in Materials Science, Dordrecht, 2007, vol. 100, pp. 1–18.
4 T. S. Qureshi and A. Al-Tabbaa, *Smart Mater. Struct.*, 2016, **25**, 084004.
5 M. Roig-Flores, F. Pirritano, P. Serna and L. Ferrara, *Constr. Build. Mater.*, 2016, **114**, 447–457.
6 S. Fan and M. Li, *Smart Mater. Struct.*, 2015, **24**, 015021.
7 D. Snoeck, L. Pel and N. De Belie, *Sci. Rep.*, 2020, **10**, 1–6.
8 Z. Li, L. R. de Souza, C. Litina, A. E. Markaki and A. Al-Tabbaa, *Mater. Des.*, 2020, **190**, 108572.
9 Z. Li, L. R. de Souza, C. Litina, A. E. Markaki and A. Al-Tabbaa, *Materials*, 2019, **12**, 3872.
10 E. Tziviloglou, V. Wiktor, H. M. M. Jonkers and E. Schlangen, *Constr. Build. Mater.*, 2016, **122**, 118–125.
11 L. Tan, B. Reeksting, V. Ferrandiz-Mas, A. Heath, S. Gebhard and K. Paine, *Constr. Build. Mater.*, 2020, **257**, 119501.
12 J. Y. Wang, H. Soens, W. Verstraete and N. De Belie, *Cem. Concr. Res.*, 2014, **56**, 139–152.
13 B. Balzano, J. Sweeney, G. Thompson, C. L. Tuinea-Bobe and A. Jefferson, *Eng. Struct.*, 2021, **226**, 111330.
14 H. Huang, G. Ye and Z. Shui, *Constr. Build. Mater.*, 2014, **63**, 108–118.
15 A. Kanellopoulos, P. Giannaros and A. Al-Tabbaa, *Constr. Build. Mater.*, 2016, **122**, 577–593.
16 P. Giannaros, A. Kanellopoulos and A. Al-Tabbaa, *Smart Mater. Struct.*, 2016, **25**, 084005.
17 K. Van Tittelboom and N. De Belie, *Materials*, 2013, **6**, 2182–2217.
18 X. Wang, Y. Huang, Y. Huang, J. Zhang, C. Fang, K. Yu, Q. Chen, T. Li, R. Han, Z. Yang, P. Xu, G. Liang, D. Su, X. Ding, D. Li, N. Han and F. Xing, *Constr. Build. Mater.*, 2019, **220**, 90–101.
19 M. Al-Ansari, A. G. Abu-Taqa, M. M. Hassan, A. Senouci and J. Milla, *Constr. Build. Mater.*, 2017, **149**, 525–534.
20 A. Beglarigale, Y. Seki, N. Y. Demir and H. Yazıcı, *Constr. Build. Mater.*, 2018, **162**, 57–64.
21 A. Kanellopoulos, P. Giannaros, D. Palmer, A. Kerr and A. Al-Tabbaa, *Smart Mater. Struct.*, 2017, **26**, 045025.
22 T. Han, X. Wang, D. Li, D. Li, F. Xing, J. Ren and N. Han, *Constr. Build. Mater.*, 2020, **241**, 118009.
23 W. Mao, C. Litina and A. Al-Tabbaa, *Materials*, 2020, **13**, 456.
24 Y. Ren, N. Abbas, G. Zhu and J. Tang, *Colloids Surf., A*, 2020, **587**, 124347.
25 X. Wang, P. Sun, N. Han and F. Xing, *Materials*, 2017, **10**, 20.
26 C. Litina, D. Palmer and A. Al-Tabbaa, *Engineering Research Express*, 2021, **3**, 025015.
27 L. Y. Lv, H. Zhang, E. Schlangen, Z. Yang and F. Xing, *Constr. Build. Mater.*, 2017, **156**, 219–229.
28 W. Xiong, J. Tang, G. Zhu, N. Han, E. Schlangen, B. Dong, X. Wang and F. Xing, *Sci. Rep.*, 2015, **5**, 10866.
29 Y. Wang, G. Fang, W. Ding, N. Han, F. Xing and B. Dong, *Sci. Rep.*, 2015, **5**, 18484.
30 N. Xu, Z. Song, M. Z. Guo, L. Jiang, H. Chu, C. Pei, P. Yu, Q. Liu and Z. Li, *Cem. Concr. Compos.*, 2021, **118**, 103951.
31 L. Souza and A. Al-Tabbaa, *Constr. Build. Mater.*, 2018, **184**, 713–722.
32 P. W. Chen, G. Cadisch and A. R. Studart, *Langmuir*, 2014, **30**, 2346–2350.
33 M. B. Romanowsky, A. R. Abate, A. Rotem, C. Holtze and D. A. Weitz, *Lab Chip*, 2012, **12**, 802–807.
34 T. Nisisako, T. Ando and T. Hatsuzawa, *Lab Chip*, 2012, **12**, 3426–3435.
35 H.-H. Jeong, Z. Chen, S. Yadavali, J. Xu, D. Issadore and D. Lee, *Lab Chip*, 2019, **19**, 665–673.
36 A. Ofner, I. Mattich, M. Hagander, A. Dutto, H. Seybold, P. A. Rühs and A. R. Studart, *Adv. Funct. Mater.*, 2019, **29**, 1806821.
37 S. Nawar, J. K. Stolaroff, C. Ye, H. Wu, D. T. Nguyen, F. Xin and D. A. Weitz, *Lab Chip*, 2020, **20**, 147–154.
38 A. Chu, D. Nguyen, S. S. Talathi, A. C. Wilson, C. Ye, W. L. Smith, A. D. Kaplan, E. B. Duoss, J. K. Stolaroff and B. Giera, *Lab Chip*, 2019, **19**, 1808–1817.
39 S. A. Damiati, D. Rossi, H. N. Joensson and S. Damiati, *Sci. Rep.*, 2020, **10**, 19517.
40 S. L. Anna, N. Bontoux and H. A. Stone, *Appl. Phys. Lett.*, 2003, **82**, 364.
41 Y. Hennequin, N. Pannacci, C. P. de Torres, G. Tetradis-Meris, S. Chapuliot, E. Bouchaud and P. Tabeling, *Langmuir*, 2009, **25**, 7857–7861.
42 P. W. Chen, R. M. Erb and A. R. Studart, *Langmuir*, 2012, **28**, 144–152.
43 A. Kanellopoulos, T. S. Qureshi and A. Al-Tabbaa, *Constr. Build. Mater.*, 2015, **98**, 780–791.
44 S. S. Datta, S.-H. Kim, J. Paulose, A. Abbaspourrad, D. R. Nelson and D. A. Weitz, *Phys. Rev. Lett.*, 2012, **109**, 134302.
45 T. Cubaud and T. G. Mason, *Phys. Fluids*, 2008, **20**, 053302.
46 J. K. Nunes, S. S. H. Tsai, J. Wan and H. A. Stone, *J. Phys. D: Appl. Phys.*, 2013, **46**, 114002.
47 J. Borrello, P. Nasser, J. C. Iatridis and K. D. Costa, *Addit. Manuf.*, 2018, **23**, 374–380.